Preparation and optical properties of Na$^+$/Eu^{3+} Co-doped CaO-WO$_3$-SiO$_2$ transparent glass-ceramics

QINLEI WEI[a], CHAOYU MA[a], MENGJIE ZHAO[a], GUOZHONG REN [a], CHUNHUI SU[a,b,*]

[a]*School of Physics. Changchun Normal University, Changchun 130031, China*
[b]*School of Material Science and Engineering, Changchun University of Science and Technology, Changchun 130022, China*

Eu^{3+} doped CaO-WO$_3$-SiO$_2$ transparent glass-ceramics were prepared by melting crystallization method, and characterized by differential scanning calorimetry (DSC), scanning electron microscopy (SEM), X-ray diffraction (XRD) and fluorescence spectroscopy. The heat treatment conditions of glass ceramics were determined. The crystal phase of glass ceramics is CaWO$_4$ (41-1431). As the crystallization time increased, the content and the size of crystals increased and the crystal shape transformed from sphere to irregular polyhedron and small amount of hexagon. Eu^{3+} doped CaO-WO$_3$-SiO$_2$ glass ceramics show strong red light emission. According to the effect of Eu^{3+} as ion microprobe, it was confirmed that Eu^{3+} has already entered the crystalline field. Under the same heat treatment conditions, the strongest intensity of luminescence was obtained with 5wt% of Eu^{3+} doped. The effect of Na$^+$ on luminescent properties of the glass-ceramics was also investigated and it was proved that Na$^+$ was helpful to efficiency of the luminescence.

1. Introduction

Glass ceramics not only possess excellent mechanical strength and chemical stability, but it also characterized by high rare earth ions doping concentration and high transparency. Rare earth doped silicate glass ceramics have became a hotspot of research due to their excellent luminescence properties. Among various rare earth ions, Eu^{3+} was widely used in red light emitting materials owing to the strong luminescence intensity and high color purity. In recent years, a lot of attention has been concentrated on the synthesis, properties and application of tungstate [1]. The calcium tungstate crystal is a good kind of laser matrix with excellent physical and luminescent stability [2].

In recent years, investigations of chemical synthesis of rare earth ions doped calcium tungstate powders have attracted much attention. Formation of Eu^{3+} doped CaWO$_4$ phosphor powder by using high temperature solid phase synthesis method was reported by Feng Liang [3], which concertrated on energy transfer between WO$_4^{2-}$ ions and Eu^{3+} ions. Ho^{3+}/Yb^{3+}/Tm^{3+} doped CaWO$_4$ crystal by using czochralski method was reported by Yanling Xu [4]. Tungstate glass by using melting method was reported by Yong Wang [5]. Tungstate glasses have been researched widely in the past few decades and the tungstate glass ceramics were seldom reported [6-15]. In this paper, Eu^{3+} doped CaO-WO$_3$-SiO$_2$ transparent glass-ceramics were achieved by melt-crystallization method. The phase compositions, surface morphologies, transmittances and luminescent properties were systematically characterized. The effect of doping concentrations of Eu^{3+} and Na$^+$ on the luminescent property were emphatically investigated.

2. Experimental section

2.1. Chemicals and equipments

Tungsten trioxide, sodium fluoride, anhydrous sodium carbonate, silica, calcium carbonate, Eu$_2$O$_3$, flux agent and clarifying agents were adopted to prepare the target products. The purity of Eu$_2$O$_3$ was 99.99 %. All other reagents were analytical grade and directly used as received without further purification.

Electronic balance, ball mill, platinum crucible, silicon molybdenum resistance furnace (16 kW), box type resistance furnace (5 kW), box gradient resistance furnace (5 kW) were used in this study.

2.2. Preparation of Eu^{3+} doped CaO-WO$_3$-SiO$_2$ transparent glass-ceramics

A melt-crystallization method was used, and the precursor materials were mixed according to the

following mass percentages: 30 % of $CaCO_3$, 10 % of WO_3, 40 % of SiO_2, 10% of H_3BO_3, 8.5 % of NaF, 0.5 % of Sb_2O_3 and 1 % of Eu_2O_3. 50 g of the mixed materials were placed in a corundum crucibles and melted at 1200 °C for 1h in resistance furnace with the heating rate of 2°C/min, and then the system was heated up to 1400 °C for 2 h under stirring. Subsequently, then melt was poured into a mold, followed by annealing at 450°C for 2 hours to obtain the as-made glass precursors. After a certain heat treatment process, the samples were transformed into glass ceramic. Finally, the samples were cut into small pieces with the size of 10 mm×10 mm×3 mm and polished.

2.3. Characterization

DSC of matrix glass samples was carried out at the temperature range of 200 °C to 1200 °C with the heating rate of 10 °C/min by using SDT2960 thermal analyzer. X-ray diffraction measurements were performed by Japan Rigaku 2500PC with Cu-K$_{\alpha 1}$ radiation at scanning rate of 4 °/min to analyze crystal composition of the glass ceramic samples. The microscopic structures of samples were observed by a SPI3800N scanning electron microscope produced by Japanese SII. Fluorescence spectra of samples were tested by using high resolution laser spectroscopy with the model of Fl9000 produced by British BIO-RAID company, with measurement range of 400 nm-700 nm.

3. Results and discussion
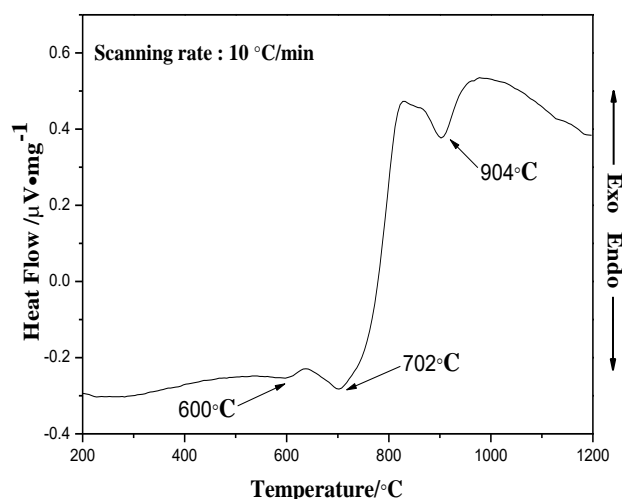
3.1. DSC analysis

Fig. 1. DSC curve of matrix glass

Fig. 1 shows the DSC curve of glass matrix. An unobvious decalescence peak at 600 °C can be observed, which indicating the transition of glass occurred. There were two obvious decalescence peaks at 702 °C and 904 °C, corresponding to the crystal growth process. A

melting phenomenon occurred when the temperature rose to 960 °C. The heat treatment system of glass ceramics are shown in Table 1.

Table 1. Heat treatment system of glass samples

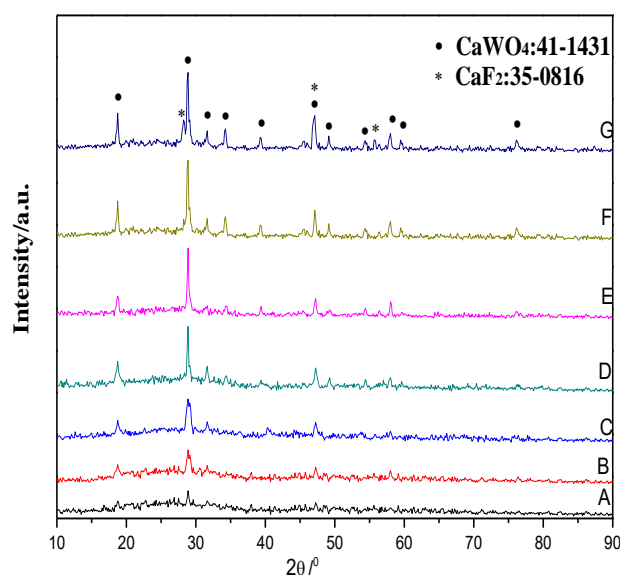| Samples No.	For crystallization
A	750 °C×30 min
B	750 °C×50 min
C	750 °C×70 min
D	750 °C×90 min
E	830 °C×50 min
F	880 °C×50 min
G	930 °C×50 min

3.2. XRD analysis

Fig. 2. XRD patterns of glass ceramic samples under different heat treatment processes (color online)

The XRD patterns of the glass ceramic samples heat-treated under different conditions are shown in Fig. 2. It demonstrated that all the diffraction peaks of samples A-E could be readily indexed to those of tetragonal phase $CaWO_4$ according to the PDF standard card No. 41-1431. Each calcium ion is surrounded by eight oxygen ions, which resulted in the distortion of original tetrahedral. Ca^{2+} ions can be easy to be substituted by rare earth ions because they existed in the tetrahedral voids. With the extension of heat treatment time or rising of temperature, the intensity of diffraction peaks of samples was increased gradually, meaning that the crystalline degree of them was increased. As the temperature reached up to 930 °C, CaF_2 (PDF No. 35-0816) was formed.

3.3. SEM observation

Fig. 3 shows the SEM images of samples A-F. As is shown in Fig. 3, the crystalline phase of sample A appeared which radius is small as well as less content of crystal and low degree of crystallization. With the increase of heat treatment time, the crystal content in samples B-D increased gradually and the size of particles became larger. The $CaWO_4$ crystals in sample B are round in morphology, and with the increase of crystallization time, crystals kept growing constantly, resulting in that some irregular shaped crystals appeared in sample C. The growth of crystal in sample D is more completed, leading to the fact that the crystals grew to some large-sized irregular polygons with a few of $CaWO_4$ hexagon crystals. With the increase of

heat-treatment temperature, a large amount of crystals can be observed in sample E, and the crystals grew slower. Agglomeration phenomenon can be evidently seen in sample F. As a conclusion, the effect of heat treatment temperature on the growth of crystal is significant. The growth of the grains in the glass ceramics is influenced by the heat treatment temperature and time. It can be seen from the SEM images, the grains gradually grow into an irregular shape from the spherical shape and the hexagonal shape appears. It shows that the grain grows gradually and does not grow completely, so there are different shapes of grains.
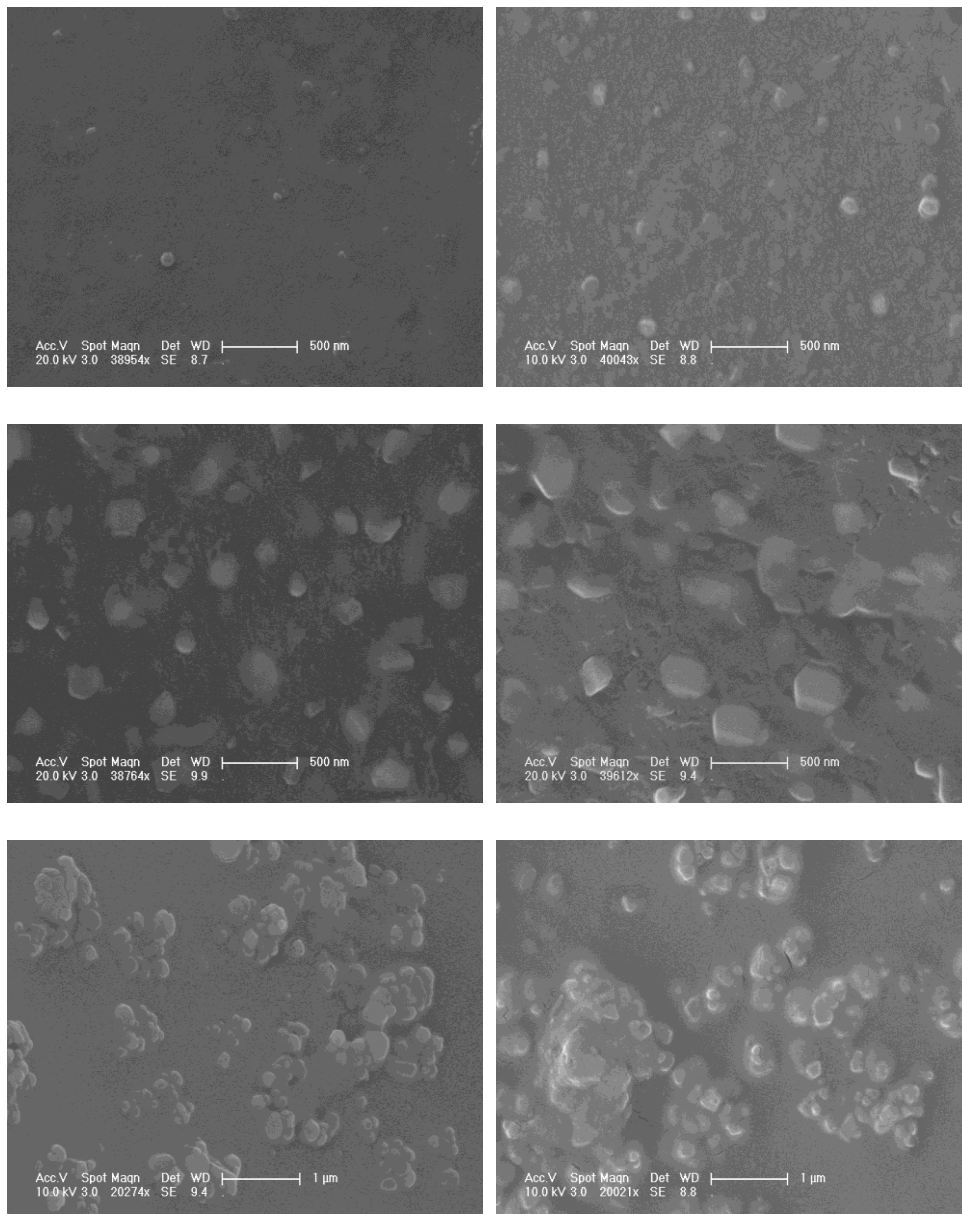

Fig. 3. SEM micrographs of glass ceramics samples
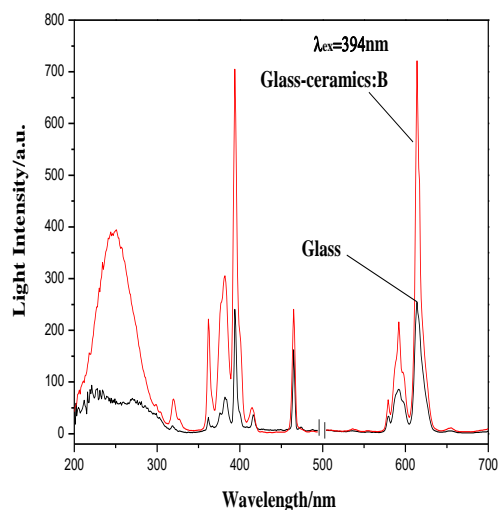
3.4. Fluorescence spectra analysis

*Fig. 4. Spectra of Eu^{3+} doped glass matrix
and glass ceramics (color online)*

Fig. 4 shows the spectra of Eu^{3+} doped glass and glass ceramic samples, in which the glass ceramic samples are heat treatment at 750 ℃ for 50 min. As shown in Fig. 4, in comparison with other excitation wavelength, the excitation intensity at 394 nm of glass and glass ceramics are stronger. So we choose 394 as sample excitation wavelength. Two emission peaks are determined at 592 nm and 614 nm for each sample by 394 nm ultraviolet, corresponding to $^5D_0 \rightarrow {}^7F_1$ and $^5D_0 \rightarrow {}^7F_2$ energy transfer of Eu^{3+} ions[16,17]. The structure of CaWO₄ is: Each calcium ion is surrounded by eight oxygen ions, which resulted in the distortion of original tetrahedral. Ca^{2+} ions can be easily substituted by rare earth ions because they existed in the tetrahedral voids. With the increase of crystal content, the emission intensity of glass ceramic samples was significantly higher than that of glass samples under the effect of crystal field although the two samples had the same Eu^{3+} concentration, which illustrates that the europium ions had participated into the crystal field. The fluorescence intensity ratio of glass ceramic samples at 614nm and 592nm is shown in Table 2.

*Table 2. The fluorescence intensity ratio of glass ceramic
samples at 614nm and 592nm*

Samples	A	B	C	D
I_{614}/I_{592}	2.69	2.87	3.12	3.29

Eu^{3+} ions have a probe function because the emission of Eu^{3+} is sensitive on the environment of crystal field. The peak at about 592 nm is the transition of magnetic dipoles and that at 614 nm is electric dipole transition, and the effect of crystal field on the two transitions is different [18, 19]. For the glass sample, the intensity of emission peak at 614 nm is 2.51 times higher than that at 592 nm. As we can see from Table 2, with the increase of heat treatment time, the ratio of fluorescence intensity become larger.

According to the probe function of Eu^{3+} ions, the influence of crystal field on two transitions of europium ion was different, which also proved that the Eu^{3+} ions have partly entered into the crystal field.
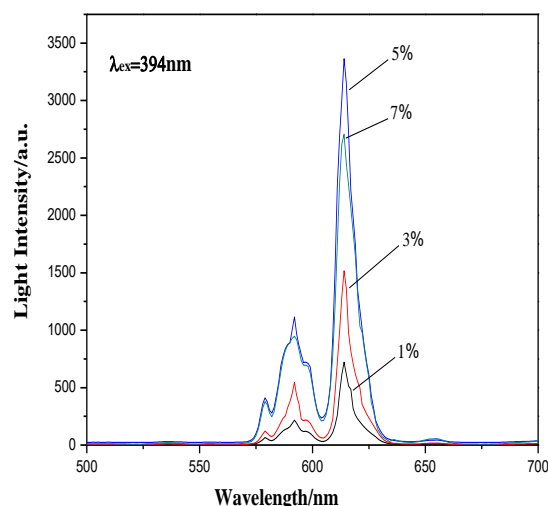

*Fig. 5. Emission spectra of different Eu^{3+} doping
concentration in glass-ceramic samples (color online)*

The fluorescence spectra of glass ceramic samples with different Eu^{3+} ions concentrations are shown in Fig. 5. The mass ratios of Eu₂O₃ were 1%, 3%, 5% and 7%, respectively. The glass ceramic samples are heat treatment at 750 ℃ for 50 min. One can see that with the increase of the Eu^{3+} ions concentration, the intensity of emission peaks increased at first and then decreased. When the Eu^{3+} ion concentration is 5%, the intensity of emission peak is the strongest.

Fig. 6 shows the effect of Na$^+$ ions on the luminescence properties of Eu^{3+} doped glass ceramic samples when the mass ratio of Eu₂O₃ is 1% and the mass ratios of Na₂CO₃ are 0 %, 2 %, 4 % and 6 %, respectively. In the same heat treatment condition, with the increase of Na$^+$ concentration, the intensity of emission peaks increased gradually, which indicated that the increase of Na$^+$ ions promoted the luminescence properties of Eu^{3+} ions. Because calcium ions are bivalent ions and rare earth ions are trivalent ions. Rare earth ions participated into the crystal by substituting calcium ions, which may result in charge defects. Charge compensation structure could be simplified by participating Na$^+$ ions into the system, because the total chemical valence of Na$^+$ ion and Ca^{2+} ion is three which is equaled with Eu^{3+} ion, thus making the europium ions are more easily participated into the crystal and improve the luminous efficiency.
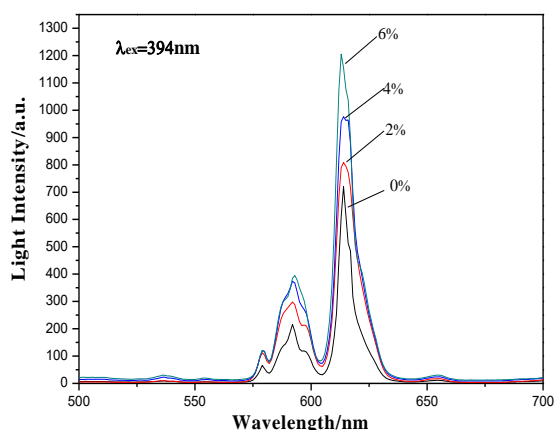
Fig. 6. Effect of Na⁺ on the spectral properties of glass ceramic samples (color online)

4. Conclusions

Eu^{3+} doped transparent $CaO\text{-}WO_3\text{-}SiO_2$ system glass ceramics containing $CaWO_4$ (41-1431) crystals were prepared and characterized. The effect of crystallization time on crystal morphology has been investigated. Crystals in samples gradually became irregular polygon from circular and emerge $CaWO_4$ crystal of hexagon shape. The Eu^{3+} ions in the glass ceramic samples were incorporated into the crystal field, and determined by the action of the probe. Emission peak of the sample was first increased and then decreased with the increase of Eu^{3+} concentration and the maximum appeared at 5wt%. And the emission spectra effects of Na^+ ions on Eu^{3+} ions were discussed and illustrate that a certain amount of Na^+ ions could improve the luminous efficiency of Eu^{3+} in the glass ceramic samples.

References

[1] Shen Xian-Fei, Gan Fu-Xi, Journal of Inorganic Materials **3**, 362 (1991).
[2] Gan Fu-Xi, Journal of the Chinese Ceramic Society **4**, 388 (1980).
[3] Liang Feng, Hu Yi-Hua, Chen Li, Acta Physica Sinica **62**, 183302 (2013).
[4] Yanling Xu, Yunlong Wang, Liansheng Shi, Optics & Laser Technology **54**, 50 (2013).
[5] Yong Wang, Tsuyoshi Honma, Takayuki Komatsu, Optical Materials **35**, 998 (2013).
[6] R. C. Pullar, S. Farrah, N. M. Alford, Journal of European Ceramic Society **27**, 1059 (2007).
[7] L. F. Johnson, G. D. Boyd, K. Nassau **50**, 87 (1962).
[8] Gao Dao-jiang, Xiao Ding-Quan, Jin Yi-Xin, Journal of Functional Materials **36**, 711 (2005).
[9] Feng-wen Kang, Yi-hua Hu, Li Chen, Journal of Luminescence **135**, 113 (2013).
[10] Ping Chen, Jiajia Zhou, Zaijin Fang, Journal of Non-Crystalline Solids **391**, 49 (2014).
[11] M. A. M. A. Maurera, A. G. Souza, L. E. B. Soledate, Materials Letters **58**, 727 (2004).
[12] Jun Ho Chung, Jung-Il Lee, Sung-Lim Ryu, Ceramics International **39**, S369 (2013).
[13] H. Althues, P. Simon, S. Kaskel, Journal of Materials Chemistry **17**, 758 (2007).
[14] C. C. Wu, K. B. Chen, C. S. Lee, Chemistry of Materials **19**, 3278 (2007).
[15] Min Li, Bin Shen, Xiangren Zhu, Rare Metal Materials and Engineering **37**, 281 (2008).
[16] Zhengwei Liu, Yingliang Liu, Dingsheng Yuan, Chinese Journal of Inorganic Chemistry **20**, 1433 (2004).
[17] Ke Wu, Le Wang, Guotang Xu, Journal of Inorganic Materials **27**, 706 (2012).
[18] Wei Xu, Chengren Li, Baojiu Chen, Acta Physica Sinica **59**, 1328 (2010).
[19] Xixian Luo, Wanghe Cao, Journal of Functional Materials **38**, 2064 (2007).

[*]Corresponding author: sch@cust.edu.cn